Available online at www.sciencedirect.com
SCIENCE DIRECT®
PERGAMON
Polyhedron 22 (2003) 1303–1313
POLYHEDRON
www.elsevier.com/locate/poly

Intervalence, electron transfer and redox properties of a triazolate-bridged ruthenium-polypyridine dinuclear complex

Reginaldo C. Rocha, Henrique E. Toma *

Instituto de Química, Universidade de São Paulo, Caixa Postal 26077, CEP 05513-970 Sao Paulo, SP, Brazil

Received 1 October 2002; accepted 4 February 2003

Abstract

A new dinuclear complex of the type *cis,cis*-$[(bpy)_2ClRu(\mu\text{-}L_b)RuCl(bpy)_2]^{n+}$ (bpy = 2,2′-bipyridine; L_b = benzotriazolate (bta); $n = 1$, 2, or 3) has been synthesized, isolated as a PF_6^- salt, and investigated in organic solutions by means of cyclic voltammetry and ultraviolet/visible/near-infrared spectroelectrochemistry. Particular emphasis has been given to the electron transfer (ET) properties of the mixed-valent species ($n = 2$), which displays a somewhat large metal–metal electronic coupling in the ground state with the complex featuring localized Ru(III) and Ru(II) oxidation states, as deduced from its intervalence charge-transfer (IVCT) band and electrochemical parameters. Analysis of the IVCT properties in the context of Hush's theory also supports a valence-trapped formulation. In spite of the class II categorization within the Robin-Day scheme, this system shows a remarkable intermetallic communication when compared with other analogues (e.g. L_b = pyrazine). Such aspect has also been stressed by comparison of the set of thermodynamic and mixed-valence parameters along with a series of L-bridged systems studied previously in aqueous solutions (in particular, $[(edta)Ru(\mu\text{-}bta)Ru(edta)]^{4-}$; edta = ethylenediamine-*N*,*N*,*N*′,*N*′-tetraacetate), and the striking differences in their intervalence characteristics have been rationalized in terms of distinct types of electronic and structural effects. Despite the contrasting behavior, the same type of superexchange mechanism ('hole-transfer') seems to prevail in all these benzotriazolate-bridged mixed-valent species. In the 2,2′-bipyridine derivative, the synergistic charge-transfer effects are the most relevant factors on the great stabilization of the mixed-valence state. The combined π-acceptor and σ,π-donor abilities of the ancillary (bpy) and bridging (bta) ligands, respectively, are also responsible for the high stability of the fully oxidized (Ru^{III}–L–Ru^{III}) and fully reduced (Ru^{II}–L–Ru^{II}) isovalent species. From the IVCT band features, the rate of intramolecular thermal ET for the mixed-valent ion was estimated on the basis of the Hush and Marcus theories.

Keywords: Benzotriazole; Electron transfer; Intervalence charge-transfer; Mixed-valence; Ruthenium-polypyridine

1. Introduction

The mixed-valence chemistry [1–3] of polynuclear transition metal systems has been extensively exploited by inorganic chemists since the late 60s, when the field was marked by the pioneering attempt by Allen and Hush [4] to organize and rationalize the properties of such materials, the formulation by Hush [5,6] of the semiclassical theory based on the perturbational donor–acceptor formalism of Mulliken [7,8], the fundamental classification of mixed-valence systems by Robin and Day [9], and the first preparations in a research laboratory of designed mixed-valent complexes by Cowan et al. [10,11] and Creutz and Taube [12,13]. Since then, polymetallic systems containing elements from virtually almost the whole three transition series have emerged, with an especial focus on the metal ions from the Group 8. Ruthenium complexes, indeed, have by far received more attention, due mainly to their desirable kinetic and thermodynamic properties (as the redox richness, for instance) derived from the low-spin d^6/d^5 electronic configuration. The literature of this class of compounds has also been continuously reviewed in the last decades [14–16]. Polypyridine complexes of ruthenium, in particular, have been more recently reviewed by Balzani et al. [17]. This type of metal-organic systems provides suitable models for the study

* Corresponding author. Tel.: +55-11-3091-3887; fax: +55-11-3815-5579.
E-mail address: henetoma@iq.usp.br (H.E. Toma).

0277-5387/03/$ - see front matter © 2003 Elsevier Science Ltd. All rights reserved.
doi:10.1016/S0277-5387(03)00105-0

of electron transfer (ET) [1] and/or energy transfer processes [18], encompassing the fundamental principles in designing prototypes of electronic and photonic devices at the molecular level with applications within the new fields of molecular nanosciences and nanotechnology [19–29].

The most important role in mediating the electronic communication in bridged mixed-valence systems is, naturally, played by the intervening bridging ligand, whose chemical nature can determine the magnitude and the mechanism of the donor–acceptor electronic interactions. In this sense, an important point was raised in our recent contributions, which involve benzotriazolate-bridged systems exhibiting stereochemical mobility [30–33]. Indeed, in a previous work [32], we reported the contrasting behavior of the intervalence transfer properties of symmetrical ruthenium-edta binuclear complexes containing benzotriazolate and benzimidazolate as bridging ligands in aqueous solutions. Because of the structural similarities of these ligands, the unexpected differences in the electronic properties were tentatively interpreted in terms of a fluxional coordination, as observed in a number of benzotriazolate complexes [34–38]. In order to improve the understanding of this type of system, we have currently extended our previous work to the benzotriazolate-bridged dimer of the 2,2′-bipyridine complex of ruthenium (Scheme 1), in which such dynamic/fluxional behavior on the bridging ligand is not observed due to the largely sterically hindered environment. The intervalence charge-transfer (IVCT) properties and the redox behavior of the dinuclear complex in organic medium were particularly explored by electrochemical and spectroelectrochemical methods and compared with related ruthenium-polypyridine dimers.

2. Experimental

2.1. Starting materials

Benzotriazole (btaH) was purchased commercially (from Aldrich) and recrystallized by slow evaporation of saturated solutions in a 3:1 ethanol/water mixture. Chemical and spectral characterizations of the neutral (btaH) ligand and the corresponding lithium salt of its anionic form (bta) are available elsewhere [31,39]. The synthesis of *cis*-$RuCl_2(bpy)_2 \cdot 2H_2O$ was based on a classical method of the literature [40]. The purity and characterization of the final product were assessed by means of elemental analysis, electronic spectroscopy and electrochemistry. Tetraethylammonium perchlorate, $(tea)ClO_4$, was prepared in accordance with standard techniques [41], recrystallized twice from hot water, and vacuum dried at 100 °C overnight. All other chemicals and organic solvents employed in the syntheses were analytical reagent grade (Aldrich, J.T. Baker, Merck or Sigma) and were used as supplied, without further purification (except for acetonitrile used as solvent in the sample solutions, which was dried and stored over 4 Å molecular sieves in a dark bottle). High purity, deionized water was obtained by passing bi-distilled water through a Nanopure™ (Barnstead) purification system.

2.2. Syntheses[1]

2.2.1. *cis,cis*-[{$Ru^{II}Cl(bpy)_2$}$_2$(bta)](PF_6)

cis-$RuCl_2(bpy)_2 \cdot 2H_2O$ (520 mg; 1.0 mmol) and benzotriazole (53.6 mg; 0.45 mmol) were suspended in 30 cm^3 of a 2:1 ethanol/water mixture. After heating to reflux for 30 min, lithium hydroxide monohydrate (21.0 mg; 0.50 mmol) was added to the reactional mixture and the reflux (under argon) continued for approximately 3 h. Following cooling to ambient temperature, the brownish red solution was filtered and vacuum dried in a rotary evaporator. The solid was then dissolved in a minimum volume of water (≈ 5 cm^3) and added dropwise into about the same volume of a stirring concentrated (1 mol dm^{-3}) aqueous solution of ammonium hexafluorophosphate, yielding a deep reddish precipitate. The product was collected on a glass frit by suction filtration, washed with a few portions of cold

[1] As a general precaution, the reactional mixtures or solutions containing bis(2,2′-bipyridine)ruthenium(II) derivatives were protected from light during the syntheses or measurements.

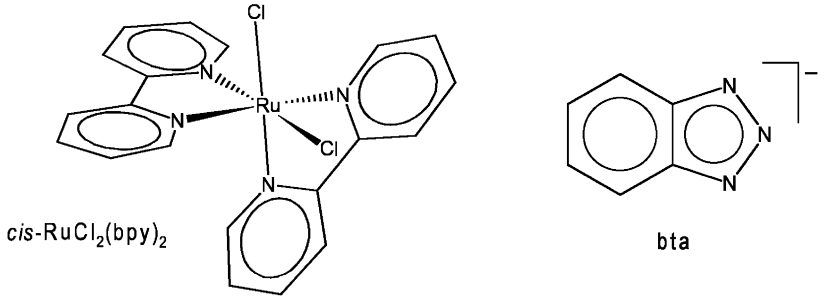

Scheme 1. Molecular precursors.

water and dried in vacuum for a couple of days in the presence of a desiccant. Further purification was performed by column chromatography, using neutral alumina (activity I; 70–300 mesh; particle size: 60–200 μm) as the filling material and acetonitrile (or, alternatively, a 10:1 acetonitrile/ethanol mixture) as the eluant. The complex collected from the large dark red band was precipitated from acetonitrile with anhydrous ethyl ether. Isolation of the final pure PF_6-salt (powdery solid) proceeded as described above. Yield: ~60%. *Anal.* Found: C, 45.3; H, 3.6; N, 12.7%. Required for $C_{46}H_{42}N_{11}O_3F_6Cl_2PRu_2$ (MW = 1214.9 g mol^{-1}): C, 45.5; H, 3.5; N, 12.7%.

2.2.2. *cis,cis-[{RuCl(bpy)$_2$}$_2$(bta)](PF$_6$)$_n$ (n = 2 or 3)*

Although the mixed-valent ($n = 2$) and the fully oxidized ($n = 3$) species were generated in situ by controlled-potential electrolysis of the fully reduced ion during the electrochemical/spectroelectrochemical measurements, their preparation by chemical oxidation of *cis,cis*-[{$Ru^{II}Cl(bpy)_2$}$_2$(bta)](PF_6) in acetonitrile solution with, respectively, 1 and 2 equiv of cerium(IV) (from either ceric ammonium nitrate or sulfate salts), were also accomplished for comparative purposes. The isolation of the solids followed the above procedure for the fully reduced monocation. Identical electrochemical and spectral data were obtained for the solutions of the oxidized complexes prepared either by this way or by electrolysis (*v. infra*). Since this work focuses on the latter (electrochemical) methods, the trivalent species were not characterized in the solid state.

2.2.3. *cis-[RuCl(bpy)$_2$(btaH)]^n*

The mononuclear protonated complex was synthesized and isolated as a hexafluorophosphate salt in the divalent state ($n = +1$), and characterized in organic solutions by electrochemical and spectroelectrochemical methods in all of its accessible oxidation states ($n = +2$, $+1$, -1), as reported recently elsewhere [34].

2.3. Physical measurements[2]

The electronic spectra in the ultraviolet (UV), visible and near-infrared (NIR) regions were recorded, respectively, on a Hewlett–Packard model 8453 diode-array spectrophotometer and on a Guided-Wave model 260 fiber-optic instrument.

Cyclic voltammograms were run with a Princeton Applied Research-PAR model 283 potentiostat (from EG&G Instruments). A conventional three-electrode arrangement consisting of a platinum working electrode, a Luggin capillary with a $Ag\,|\,Ag^+$ (1.0×10^{-2} mol dm^{-3} silver nitrate) reference electrode ($E^\circ = +0.503$ V vs. standard hydrogen electrode, SHE [42,43]) and a platinum wire as the auxiliary electrode, was used. The sample solutions were thoroughly degassed prior to beginning the experiments, and before each measurement the solutions were also purged with argon (White–Martins). Working electrodes were polished with alumina paste (Struers). Cyclic voltammograms were recorded at sweep rates of 10–1000 mV s^{-1}. The potential values given in this paper are uncorrected for junction potentials and referred vs. SHE.

Spectroelectrochemical measurements in the UV/visible region were carried out with a PAR model 366 bipotentiostat in parallel with the diode-array spectrophotometer. A three-electrode system was specially designed for a rectangular quartz cell of 0.25 mm internal optical length. A gold minigrid was used as a transparent working electrode, in the presence of a small $Ag\,|\,Ag^+$ reference electrode and a platinum auxiliary electrode. The OTTLE cell was located directly in the spectrophotometer, and the absorption change was monitored during the electrolysis.

Spectroelectrochemistry by reflectance in the NIR region was performed by using a fiber-optic probe for in situ measurements in a quartz, flat bottom, specially designed electrochemical cell. In this case, the fiber-optic probe was placed perpendicularly to the mirror surface of the platinum electrode which was kept approximately 0.2 mm from the bottom, providing a constant optical length. Tetraethylammonium perchlorate, (tea)ClO_4, was used as a supporting electrolyte (ionic strength $I = 0.10$ mol dm^{-3}) in both electrochemistry and spectroelectrochemistry.

Elemental analyses were carried out by the Microanalytical Laboratory of the Institute of Chemistry, University of São Paulo.

Molecular mechanics (MM+) and semiempirical quantum chemical (ZINDO) calculations were performed as described in details elsewhere [33,44–46].

3. Results and discussion[3]

3.1. Syntheses

One of the most important synthetical features of the starting complex $Ru^{II}Cl_2(bpy)_2$ is its ability to promptly substitute a chloride in warm organic/aqueous solutions to form $[Ru^{II}Cl(bpy)_2(S)]^+$ (Eq. (1)). This intermediate

[2] The measurements were performed at room temperature (25 ± 1 °C).

[3] Since the derivatives containing the bis(2,2′-bipyridine)-ruthenium(II/III) fragment to be mentioned hereafter are all *cis* with regard to the coordination geometry, the *cis* prefix which should appear as a notation along with the formulas is omitted in the next sections.

complex is rather labile and easily exchanges the solvent ligand in the presence of *N*-heterocyclic ligands, yielding the corresponding substituted species (Eq. (2); in this case, L is the monoionizable acid btaH ligand).

$$RuCl_2(bpy)_2 \overset{\text{alcohol/water}}{\underset{\Delta}{\rightarrow}} [RuCl(bpy)_2(S)]^+ + Cl^- \quad (1)$$

$$[RuCl(bpy)_2(S)]^+ + L \rightarrow [RuCl(bpy)_2(L)]^+ + S \quad (2)$$

In the presence of excess $Ru^{II}Cl_2(bpy)_2$ a further substitution reaction involving the coordinated ligand (L_b = bta) of the mononuclear complex takes place, as illustrated in Eq. (4). In the current example, a previous deprotonation must occur on the L (btaH) ligand in $[Ru^{II}Cl(bpy)_2(L)]^+$ to make the second coordination site available for binding (Eq. (3)). This step should be performed under an inert atmosphere, since Ru(II/III) ions are more vulnerable to oxidation in basic media.

$$[RuCl(bpy)_2(L)]^+ + OH^- \rightarrow RuCl(bpy)_2(L_b) + H_2O \quad (3)$$

$$[RuCl(bpy)_2(S)]^+ + RuCl(bpy)_2(L_b) \rightarrow [\{RuCl(bpy)_2\}_2(L_b)]^+ + S \quad (4)$$

Although purification by recrystallization in acetone/water has also been employed, the use of column chromatography as described in Section 2 led to better results in terms of yield and purity of the compounds, even though a significant amount of the product was still lost in the successive procedures, limiting the final yield to approximately 65%. Interestingly, the yields achieved for the mononuclear precursors were higher than 80% [34], indicating that the dimers are more susceptible to either dissociation or side reactions during the passage through the chromatographic column.

Unlike some similar ruthenium-polypyridine dimers bridged by π-acceptor ligands (e.g. pyrimidine [47]), both the dissolved and the isolated oxidized (mixed-valent, Ru^{III}–Ru^{II}, and isovalent, Ru^{III}–Ru^{III}) species were found to be stable to decomposition (at least within a time scale of weeks and when stored in the absence of light).

As shown in the Section 2, the elemental analyses were consistent with the dimeric formulation. Further support for this formulation comes from electrochemistry and electronic spectroscopy, as discussed in the sections below.

3.2. Electrochemistry

The cyclic voltammogram of $[\{Ru^{II}Cl(bpy)_2\}_2(bta)]^+$ in acetonitrile displays: (i) two pairs of reversible waves in the region of positive potentials, with $E_{1/2}^{(1)} = 1.34$ V and $E_{1/2}^{(2)} = 0.99$ V (both exhibiting $i_a/i_c = 1$, $\Delta E_p = 65$ mV at 100 mV s^{-1}, and $i_p \propto v^{1/2}$),[4,5] associated to the redox couples centered on the metal ions (Eq. (5) and Eq. (6)); and (ii) two poorly-resolved wave couples in the negative region of potentials ($E_c^{(1)} = -1.28$ V and $E_c^{(2)} \sim -1.52$ V), which have nearly twice the current intensity relative to those in the positive region and were related to the two closely spaced characteristic reductions of the bipyridine ligands on each ruthenium center, according to previous assignments [34,48]. Due to the inherent difficulty in estimating the half-potential ($E_{1/2}$) for these latter waves at the edge of the solvent potential window, only the cathodic peak potentials were taken into account for the ligand-centered reductions.

$$[\{Ru^{III}Cl(bpy)_2\}_2(L_b)]^{3+} + e^- \overset{[E_{1/2}^{(1)}]}{\rightleftarrows} [(bpy)_2ClRu^{III}(L_b)Ru^{II}Cl(bpy)_2]^{2+} \quad (5)$$

$$[(bpy)_2ClRu^{III}(L_b)Ru^{II}Cl(bpy)_2]^{2+} + e^- \overset{[E_{1/2}^{(2)}]}{\rightleftarrows} [\{Ru^{II}Cl(bpy)_2\}_2(L_b)]^+ \quad (6)$$

It is interesting to observe that $E_{1/2}^{(2)}$ is very close to the $E_{1/2}$ value for the monomer protonated on L (benzotriazole), $[Ru^{III/II}Cl(bpy)_2(btaH)]^{2+/+}$ (0.91 V [34]), whereas $E_{1/2}^{(1)}$ is rather more positive. Hence, the coordination of a second $\{RuCl(bpy)_2\}$ group to the deprotonated (benzotriazolate) species to give the $[\{RuCl(bpy)_2\}_2(bta)]^+$ dimer exerts nearly the same effect as a proton on the ligand. In the dimer, however, once the Ru^{II}–Ru^{II} complex is oxidized to Ru^{II}–Ru^{III} at 0.99 V, the additional positive charge is readily communicated across the bridging ligand to the other relatively remote metal moiety, making the potential for a second oxidation to yield Ru^{III}–Ru^{III} higher (more positive), with a significant redox split ($\Delta E_{1/2}$) of 0.35 V.

The potential separation between $E_{1/2}^{(1)}$ and $E_{1/2}^{(2)}$ can be used to determine the stability of the mixed-valent species with respect to the reduced and oxidized isovalent ones, by means of the calculation of K_c [49], the equilibrium constant associated to the comproportionation reaction of Eq. (7).

$$[\{Ru^{III}Cl(bpy)_2\}_2(bta)]^{3+} + [\{Ru^{II}Cl(bpy)_2\}_2(bta)]^+ \rightleftarrows 2[(bpy)_2ClRu^{III}(bta)Ru^{II}Cl(bpy)_2]^{2+} \quad (7)$$

In this way, by using the classical thermodynamic expressions [1,49], the K_c value was found to be 8.3 ×

[4] The $E_{1/2}$ values for the reversible couples were calculated from half the difference between E_p values for anodic and cathodic waves (*i.e.* $E_{1/2} = [E_a + E_c]/2$) and used as a formal reduction potential on the assumption that differences in diffusion coefficients for oxidized and reduced species are negligible.

[5] The cyclic voltammograms were essentially invariant to changes in the sweep rate in the range of 10–500 mV s^{-1}; the higher than theoretically predicted ΔE_p values (59 mV for a single-electron process) presumably arise from uncompensated solution resistance.

10^5, which corresponds to a large comproportionation driving force (ΔG_c) of -8.1 kcal mol^{-1} (2.8×10^3 cm^{-1}).[6]

3.3. Spectroelectrochemistry

The electronic spectra of $[\{RuCl(bpy)_2\}_2(bta)]^{n+}$ in its three redox states ($n = 1$, 2 or 3), which are collected and assigned in Table 1, were obtained by generation of such species by electrolysis, in situ, under application of suitable potentials in acetonitrile solutions on the basis of the cyclic voltammetric guidance. In agreement with the electrochemical results, electrode reactions were all chemically and electrochemically reversible in the spectroelectrochemistry, as revealed by the complete spectral recovery upon either reduction or oxidation processes. In addition to the metal-to-ligand charge-transfer (MLCT)/ligand-to-metal charge-transfer (LMCT) bands in the visible region, the mixed-valent species ($n = 2$) also exhibits a strong absorption above 1×10^3 nm (Fig. 1), whereas both fully reduced ($n = 1$) and fully oxidized ($n = 3$) complexes are transparent in the NIR region.

Analogously to the monomeric species studied previously [34], the visible spectra of the dimers (Table 1) are dominated by charge-transfer transitions involving the Ru(II/III) ions and the peripheral 2,2-bipyridine ligands. Absorptions associated to the bridging ligand benzotriazolate might also occur in the same region with lower intensities, whose detection would presumably be precluded by the highly intense Ru↔bpy bands [34].

The spectral properties of the ligand-bridged dimeric complexes are of interest in that they should reflect the electronic interactions between the two remote metallic centers. In the present system, except for slight shifts due to π-backbonding or π-acid/base effects on the dimers of the type $[(bpy)_2ClRu^{II,III}(bta)M]^{x+}$ (with M = $\{Ru^{II,III}Cl(bpy)_2\}^{y+}$), the UV/visible spectra of the isovalent (Ru^{II}–Ru^{II} or Ru^{III}–Ru^{III}) dinuclear species can be plausibly explained by the assignment made for the individual mononuclear complexes (i.e. where M = H; Ref. [34]). In the particular case of the mixed-valent (Ru^{III}–Ru^{II}) species, however, the spectrum is not simply the sum of the spectra of the two isolated moieties, as deduced from the comparison in Table 1. This is *per se* a strong evidence of some significant extent of electronic perturbation (*v. infra*).

[6] The dimer investigated herein has sufficiently large $\Delta E_{1/2}$ value that corrections for comproportionation to the observed extinction coefficients [50,51] were ignored.

3.4. Mixed-valence properties

The mixed-valent complex, $[(bpy)_2ClRu^{III}(bta)Ru^{II}Cl(bpy)_2]^{2+}$, was obtained by electrochemical oxidation of $[\{Ru^{II}Cl(bpy)_2\}_2(bta)]^{+}$ at 1.17 V, the average potential between $E^{(1)}_{1/2}$ and $E^{(2)}_{1/2}$. In addition to the bands at 425 and 588 nm, assigned to the MLCT and LMCT transitions involving the bpy ligands on the reduced and oxidized moieties, respectively, its NIR spectrum (Fig. 1) displays a broad ($\Delta\nu_{1/2} = 4.16 \times 10^3$ cm^{-1}) and intense ($\varepsilon = 1.35 \times 10^3$ dm^3 mol^{-1} cm^{-1}) band at $\lambda_{max} = 1460$ nm ($\lambda_{max} = 6.85 \times 10^3$ cm^{-1}), which is associated to the IVCT transition illustrated in Eq. (8).

$$[(bpy)_2ClRu^{III}(bta)Ru^{II}Cl(bpy)_2]^{2+} \xrightarrow{h\nu} [(bpy)_2ClRu^{II}(bta)Ru^{III}Cl(bpy)_2]^{2+} \quad (8)$$

On the basis of the Hush model [6] a very useful criterion to distinguish localized and delocalized mixed-valence systems is to compare the predicted and the empirical values of $\Delta\nu_{1/2}$ (the bandwidth at half-height) for the intervalence band. In this current case, the theoretical value of the IVCT bandwidth, calculated by the formula $\Delta\nu_{1/2} = (2310 \times \lambda_{max})^{1/2}$ (for a symmetrical system at 298 K [1,6]), is 3.98×10^3 cm^{-1}. As a consequence of the validity of the '$\Delta\nu^{(exp)}_{1/2}/\Delta\nu^{(calc)}_{1/2} \geqslant 1$' relationship (*v. supra*), this system is better described by the class II within the scope of Robin and Day's categorization [9] and, therefore, the classical expressions of Hush (Eq. (9) and Eq. (10)) for a *Gaussian*-shaped band in a two-level system [1,6] are applicable to the estimation of H_{AB} and α^2, which are the electronic coupling (resonance energy or electron exchange matrix element) and the electron delocalization parameters for the ground state, respectively.

$$H_{AB}(\text{in cm}^{-1}) = \frac{2.05 \times 10^{-2}}{d}(\bar{\nu}_{max} \cdot \varepsilon_{max} \cdot \Delta\bar{\nu}_{1/2})^{1/2} \quad (9)$$

$$\alpha = \frac{H_{AB}}{\bar{\nu}_{max}} \quad (10)$$

The equations above are derived from the oscillator strength and energy of the IVCT band, and the donor–acceptor separation; the quantities $\lambda_{max} = E_{op}$ and $\Delta\nu_{1/2}$ are given in inverse centimeters, ε_{max} is the molar extinction coefficient, and d is the distance in angstroms.

By assuming an ET distance (d) of 5.9 Å, which is actually the theoretical geometric metal–metal separation calculated through hybrid molecular mechanics/quantum semiempirical methods (see Section 2), H_{AB} and α^2 were determined to be 680 cm^{-1} and 9.9×10^{-3}, respectively. Even though this system evidently features localized Ru(III) and Ru(II) oxidation states with just slight delocalization (since only 1% of the odd electron is

Table 1
UV–Vis spectral data for some 2,2′-bipyridine complexes of ruthenium

Complex	MLCT λ/nm ($\varepsilon/10^3$ M^{-1} cm^{-1})	LMCT λ/nm ($\varepsilon/10^3$ M^{-1} cm^{-1})	Intraligand ($\pi\rightarrow\pi^*$) λ/nm ($\varepsilon/10^4$ M^{-1} cm^{-1})
cis-$Ru^{II}Cl_2(bpy)_2$ [a]	380 (8.8); 553 (9.1)		243 (2.1); 297 (5.0)
cis-$[Ru^{III}Cl_2(bpy)_2]^+$ [a]		380 (5.6)	298 (2.5); 310 (2.2)
cis-$[Ru^{II}Cl(bpy)_2(btaH)]^+$ [b]	347 (8.5); 465 (5.7)		242 (2.0); 290 (4.0)
cis-$[Ru^{III}Cl(bpy)_2(btaH)]^{2+}$ [b]		423 (3.5)	248 (2.1); 288 (2.4)
cis,cis-$[(bpy)_2ClRu^{II}(bta)Ru^{II}Cl(bpy)_2]^+$	344 (8.9); 464 (5.9)		242 (2.6); 289 (4.5)
cis,cis-$[(bpy)_2ClRu^{II}(bta)Ru^{III}Cl(bpy)_2]^{2+}$	425 (5.2)	588 (3.2)	244 (2.4); 288 (3.9)
cis,cis-$[(bpy)_2ClRu^{III}(bta)Ru^{III}Cl(bpy)_2]^{3+}$		455 (3.4); 640 (2.0)	247 (2.7); 299 (2.8)

[a] Ref. [52].
[b] Ref. [34].

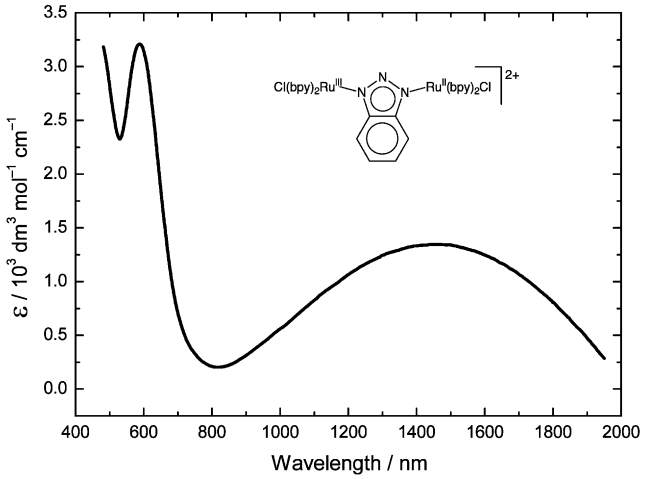

Fig. 1. Electronic spectrum of the mixed-valent *cis,cis*-$[(bpy)_2ClRu(\mu\text{-}bta)RuCl(bpy)_2]^{2+}$ complex, under 1.2 V, in CH_3CN ($I = 0.10$ mol dm^{-3} (tea)ClO_4).

shared by either metal centers), the magnitude of the electronic interaction is remarkable for this type of complex. This can be inferred by the illustrative comparison with the pyrazine- [53,54] and the pyrimidine-bridged [47] counterparts, $[(bpy)_2ClRu^{III}(L_b)\text{-}Ru^{II}Cl(bpy)_2]^{3+}$ (L_b = pz or pym), for which the values of H_{AB} are 390 and ~ 125 cm^{-1}, respectively (both with a discrete K_c of $\sim 10^2$). It is also important to notice that, within the experimental error, the intermetallic distance in the pyrimidine derivative (6.0 Å) is the same as the benzotriazolate's (5.9 Å), indicating that the main factor involved in the promotion of the electronic communication in such systems is indeed the electronic character of the intervening ligand in providing efficient $d\pi(M^{II})$–$\pi/\pi^*(L_b)$–$d\pi(M^{III})$ orbital conjugation and not only the donor–acceptor distance. These results reinforce the previous conclusions [30–33,39,55] on the striking properties of benzotriazolate as a very efficient conductor (electron-rich) bridging linker.

A relevant comparison to be emphasized in this work involves the symmetrical $[(edta)Ru(bta)Ru(edta)]^{4-}$ complex [31,32]. By comparing the IVCT band properties of this ion ($\lambda_{max} = 6.9\times10^3$ cm^{-1}; $\varepsilon = 2.2\times10^3$ dm^3 mol^{-1} cm^{-1}; $\Delta\nu_{1/2} = 2.8\times10^3$ cm^{-1}; solvent-independent) with those of $[(bpy)_2ClRu(bta)RuCl(bpy)_2]^{2+}$, it is concluded that there is a rather larger electronic coupling and delocalization for the former ion, and that it is clearly outside the weak/moderate interaction to which the Hush theory applies. For instance, the experimental $\Delta\nu_{1/2}$ value for the polypyridine complex matches very favorably the value predicted by Hush theory, with a ratio close to unity ($\Delta\nu_{1/2}^{(exp)}/\Delta\nu_{1/2}^{(calc)} = 1.05$). In the case of the related edta-containing derivative, on the contrary, $\Delta\nu_{1/2}$ found experimentally is far narrower than the (over)estimated value ($\Delta\nu_{1/2}^{(exp)}/\Delta\nu_{1/2}^{(calc)} = 0.70$; Refs. [31,32]). The possible reasons for such a contrasting behavior are outlined below.

As pointed out in Section 1, since the dimeric ruthenium-polypyridine systems have well-developed chemistry, their mixed-valence properties can be explored as a function of chemical modification effects. One of the most important variations is focused on the bridging ligand, which is capable to determine the extent of electron delocalization in the ground state and define the type of mechanism involved in the electron exchange [56]. In the $[(bpy)_2ClRu(L_b)RuCl(bpy)_2]^{n+}$ dimers containing cationic or neutral π-acceptor L_b, the most likely orbital pathway for Ru(II)–Ru(III) interaction is through the mixing of $d\pi(Ru^{II})$ and $d\pi(Ru^{III})$ with unoccupied $\pi^*(L_b)$ orbitals, which characterizes the so-called ET mechanism. On the other hand, if the dimer contains a neutral or anionic σ,π-donor L_b, the major pathway for the intermetallic electronic interaction is through the mixing of the $d\pi$ levels of the terminal donor (reduced) and acceptor (oxidized) metal ions and

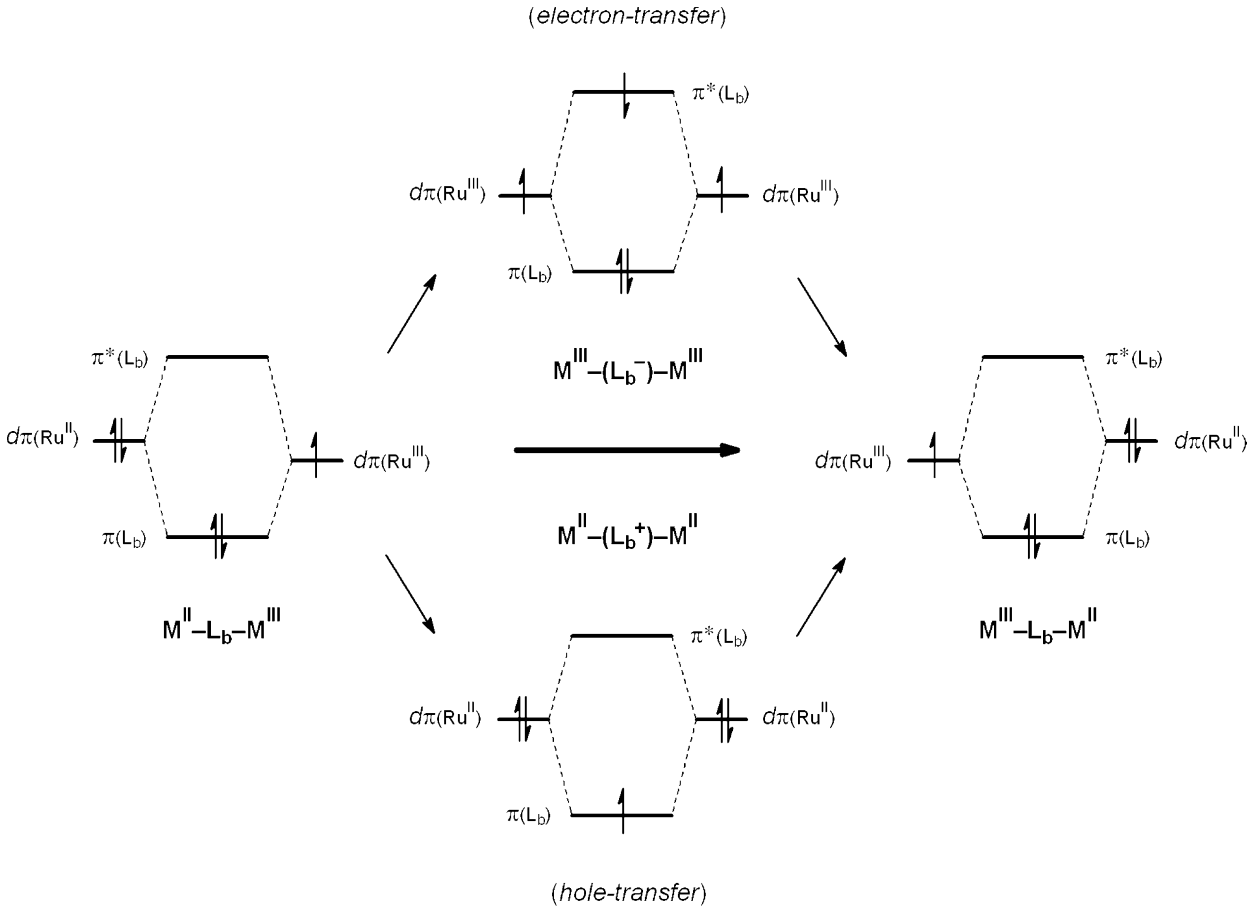

Scheme 2. Qualitative orbital diagram illustrating superexchange pathways for bridge-mediated metal–metal interactions: ET via the π* LUMO of the bridging ligand (top); and hole-transfer via the π HOMO of the bridging ligand (bottom).

the filled π orbitals of L_b, leading to a hole-transfer mechanism (Scheme 2).[7,8]

The electron delocalization of the type $d\pi$–$d\pi$ across the π-system of L_b might be expected to be necessarily less for the $\{Ru(bpy)_2\}$ groups than for the {Ru(edta)} groups because of (i) the extensive $d\pi \rightarrow \pi^*$ backbonding with the peripheral bpy ligands and (ii) the electron-donor character of edta, which makes the Ru ions much richer in charge density and therefore would favor the delocalization across the benzotriazolate ligand. However, since the same type of exchange mechanism must prevail in both ethylenediaminetetraacetate and 2,2′-bipyridine ruthenium dimers bridged by benzotriazolate (based on systematic analysis of charge-transfer energies; $E_{MLCT} >> E_{LMCT}$), and assuming that both complexes are subject to the same coordination modes and metal–metal geometric distance, then, $[(bpy)_2ClRu^{II}(bta)Ru^{III}Cl(bpy)_2]^{2+}$ should display even greater electronic coupling than $[(edta)Ru^{II}(bta)Ru^{III}(edta)]^{4-}$. This conclusion is based on the fact that bpy is a typical π-acceptor/acid ancillary ligand and, hence, would promote a better energy match between the metallic $d\pi$ orbitals and the energetic π occupied orbitals of the σ,π-donor/basic bridging ligand (bta). The edta co-ligand, in turn, has donor coordinating (carboxylate) groups which make the energy of the ruthenium $d\pi$ orbitals higher and, consequently, would increase the energy separation between $d\pi$ and $\pi(L_b)$ levels and decrease the degree of metal-L_b-metal orbital mixing through a hole-transfer mechanism.

Once the above hypothesis is not confirmed experimentally, an alternative model based on a dynamic coordination on the bridging ligand is reinforced. This is particularly important in the case of the [(edta)Ru-

[7] The bridge-mediated electron transfer (which takes advantage of the lowest unoccupied molecular orbitals—LUMOs—of the bridging ligand) and hole transfer (which takes advantage of the highest occupied molecular orbitals—HOMOs—of the bridging ligand) mechanisms are based on superexchange theory [57], an approach which considers overlap between metal orbitals mediated by through-bond interactions across the bridging ligand.

[8] For instance, molecular orbital (ZINDO) calculations [33,44–46] on the free benzotriazolate and pyrazine ligands show that for bta the highest π and the lowest π* orbital energy levels are 5.2 and 4.0 eV higher compared to pz. In addition, the partial charges localized at the nitrogen atoms are, as expected, lower for pz ($\delta q > 0.1$/N).

(bta)Ru(edta)]$^{4-}$ species, whose structural arrangement enables a symmetrical approximation of the ruthenium-edta moieties toward each other via a fluxional binding mode of the type M–[η^2-(N1,N2)bta(N2,N3)-η^2]–M [31,32]. According to a theoretical analysis, this type of interaction would involve some extent of direct orbital overlap through the intermediate N2 nitrogen atom of benzotriazolate, i.e. (M)d–p(N2)p–d(M), in addition to the expected edge-to-edge interaction through the 'rigid' mode involving the two terminal N1 and N3 coordinating sites [31,32]. In contrast, the same coupling enhancement effect seems not to exist in [(bpy)$_2$ClRu^{II}-(bta)Ru^{III}Cl(bpy)$_2$]$^{2+}$, as deduced from its mixed-valence behavior when compared to the edta counterpart. One of the main reasons for these contrasting properties was provided by molecular modeling and quantum (semiempirical level) calculations (see Section 2 for details), which indicated a high degree of sterical hindrance involving the neighbor hydrophobic polypyridine bulks and also the electrostatic repulsion between the chloride ligands from each {RuCl(bpy)$_2$} moiety, precluding an 'extra' coupling based on a metal–metal distance shortening from the fluxionality of the bridging ligand. In this case the intermetallic communication most likely propagate across the benzotriazolate by 'usual' orbital conjugation involving the two extreme binding sites on the bridge [i.e. (M)d_π–p_π(N1)bta(N3)p_π–d_π(M)], analogously to the observed in linear, symmetrical two-site bridging ligands such as pyrazine.

Even though the degree of electronic interaction in the polypyridine derivative is clearly less pronounced than in the analogue with edta, it is noticeable that the H_{AB} value for [(bpy)$_2$ClRu^{II}(bta)Ru^{III}Cl(bpy)$_2$]$^{2+}$ is superior to the majority of similar literature examples involving either π-acid (usually neutral) or σ,π-basic (usually anionic) bridging ligands. In this sense, an interesting comparison of some relevant key parameters is provided in Table 2 for both edta and bpy complexes of ruthenium bridged by benzotriazolate and pyrazine.

3.5. Electron transfer

One of the main reasons for interest in mixed-valent molecules is the possibility that their intervalence transitions can be exploited to assess rate constants and activation barriers for thermal intramolecular ET between separated redox sites [59], since the measurement of interchange rate constants directly has proven to be rather difficult.

An illustrative manner of describing optically-induced (Franck–Condon) and thermally-induced ET metal-to-metal electronic transitions in mixed-valence systems is

Table 2
Comparative thermodynamic and electronic parameters for some bpy and edta symmetrical dimers containing benzotriazolate or pyrazine as bridging ligands

Complex	$\Delta vE_{1/2}$ (V)	K_c	λ_{max} (cm^{-1})	ε_{max} (M^{-1} cm^{-1})	$\Delta\lambda_{1/2}$ (exp) (cm^{-1})	$\Delta\nu_{1/2}$ (calc) (cm^{-1})	d (Å)	α^2	H_{AB} (cm^{-1})	Class
[(bpy)$_2$ClRu(bta)RuCl(bpy)$_2$]$^{2+}$ [a]	0.35	8.3×10^5	6.85×10^3	1.35×10^3	4.16×10^3	3.98×10^3	5.9	9.9×10^{-3}	680	II
[(bpy)$_2$ClRu(pz)RuCl(bpy)$_2$]$^{3+}$ [b]	0.12	1.0×10^2	7.69×10^3	0.45×10^3	4.90×10^3	4.22×10^3	6.9	2.6×10^{-3}	390	II
[(edta)Ru(bta)Ru(edta)]$^{4-}$ [c]	0.20	2.4×10^3	6.90×10^3	2.20×10^3	2.85×10^3	4.00×10^3	>4.4; <5.7	>0.012; <0.25	>780; <3450	II–III/III
[(edta)Ru(pz)Ru(edta)]$^{3-}$ [d]	0.14	2.4×10^2	10.3×10^3	0.24×10^3	4.70×10^3	4.88×10^3	6.8	9.9×10^{-4}	320	II

[a] This work.
[b] Ref. [53].
[c] Ref. [30].
[d] Refs. [16,58].

by using bidimensional configurational-coordinate energy diagrams,[9] as introduced by Hush [6,60]. Such a qualitative diagram is shown in Scheme 3 for a symmetrical system like $[(bpy)_2ClRu^{II}(bta)Ru^{III}Cl(bpy)_2]^{2+}$ (i.e. where the net free energy change following the ET reaction—driving force, ΔG^0—is zero). The important relationships among the various parameters in Scheme 3 are elucidated hereafter, along the discussion below.

On the basis of the magnitude of H_{AB} for this system, one can conclude that the electronic coupling between the donor (Ru^{II}) and acceptor (Ru^{III}) redox sites is sufficient that the related thermal ET reaction of Eq. (11) is totally adiabatic in the sense used within Marcus' semiclassical kinetic theory of ET [61–66].

$$[(bpy)_2ClRu^{II}(bta)Ru^{III}Cl(bpy)_2]^{2+} \xrightarrow{k_{ET}} [(bpy)_2ClRu^{III}(bta)Ru^{II}Cl(bpy)_2]^{2+} \quad (11)$$

According to this approach, the rate for intramolecular ET processes is given by Eq. (12) [67]. In the adiabatic, symmetrical case represented in Eq. (11) and Scheme 3, the adiabaticity factor κ is unity (i.e. tunneling through the activation barrier is completely unimportant) and λ is the free energy term corresponding to the reorganizational energy[10] which, in turn, can be approximate as E_{op} or λ_{max}, the energy involved in the optically-induced IVCT transition). At last, in the high-temperature limit (i.e. $k_BT >> h\omega$; where k_B and h are Boltzmann's and Planck's constants, respectively), the pre-exponential factor ν_n (nuclear frequency factor for the rate of thermal intramolecular ET, which includes both solvent response and inner-sphere bond reorganizations required by ET between the localized valence states) is commonly assumed to be 5×10^{12} s^{-1} in the working conditions used [16].[11]

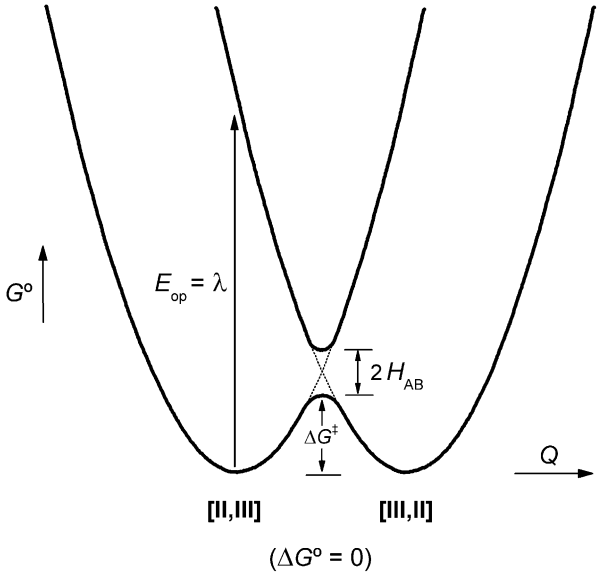

Scheme 3. Qualitative diagram of free energy vs. nuclear coordinates for the ET reaction in a symmetric, charge-localized mixed-valent complex of the type $[(bpy)_2ClRu(bta)RuCl(bpy)_2]^{2+}$.

$$k_{ET} = \kappa \cdot \nu_n \exp\left[-\left(\frac{\Delta G^*}{RT}\right)\right] \quad (12)$$

As a matter of fact, the equation above must take explicitly into account the resonance energy leading to the splitting of $2H_{AB}$ between the upper and lower 'surfaces' in Scheme 3, resulting the following expression for the thermal activation barrier:

$$\Delta G^* = \lambda/4 - H_{AB} + H_{AB}^2/\lambda \quad (13)$$

By making the typical assumptions above, the ET rate for the mixed-valent dimer $[(bpy)_2ClRu^{III}(bta)Ru^{II}Cl(bpy)_2]^{2+}$ at 298 K was calculated using Eq. (12) and Eq. (13) to yield $k_{ET} = 2.5 \times 10^{10}$ s^{-1}, which is in reasonable agreement with values obtained for similar through-bridge moderately coupled (class II) systems in the literature. For instance, k_{ET} for the pyrazine analogue, $[(bpy)_2ClRu(pz)RuCl(bpy)_2]^{3+}$ (in acetonitrile at 298 K), was estimated to be $\sim 10^{10}$ s^{-1} [16,53,54], based on the same type of optical measurements here reported. The higher value for the benzotriazolate-bridged derivative is mainly due to its lower activation barrier which, in turn, is a consequence of the more pronounced electronic coupling [H_{AB} (bta) = 680 cm^{-1}; H_{AB} (pz) = 390 cm^{-1}].

As for the Ru(edta) derivative, its high degree of electronic coupling suggests that it approaches the delocalized (class III) behavior, where the ET rate is expected to be exceptionally fast and so the semiclassical treatment above is no longer applicable. If it is assumed that the $[(edta)Ru(bta)Ru(edta)]^{4-}$ dimer is fully delocalized (class III), then the intramolecular ET is barrierless and k_{ET} approaches the maximum theoretical

[9] These diagrams actually represents a plane drawn through a multidimensional, energy-coordinate surface along a generalized nuclear (or reaction) coordinate which is sensitive to changes in oxidation state at both terminal metal centers upon the surrounding coordination and solvent spheres. The coupled vibrations or librations are treated classically as harmonic oscillators. Such structural changes as a function of the metallic redox states changes are indeed responsible for the resulting electron transfer activation barrier, at the top of which both donor and acceptor moieties have the same configuration in order to promote the electron exchange.

[10] The reorganizational energy indeed includes components from both inner-sphere (molecular vibrations) and outer-sphere (solvent reorientation/polarization) reorganizations; *i.e.*, $\lambda = \lambda_i + \lambda_o$. For a more detailed examination of these parameters, see, for instance, Refs. [1,6,16,59].

[11] This means that the theoretical maximum rate constant can approach the nuclear frequency factor, ν_n (10^{12}–10^{13} s^{-1}), for barrierless electron transfer (i.e. in delocalized systems with $H_{AB} \geqslant \lambda/2$).

value, whose magnitude is about the nuclear frequency (see footnote #9).[12]

4. Concluding remarks

In the mixed-valence ion *cis,cis*-$[(bpy)_2ClRu(\mu\text{-}bta)RuCl(bpy)_2]^{2+}$ there is experimental evidence for discrete Ru(III) and Ru(II) valences and slight delocalization. Even so, the key parameter for electronic coupling, H_{AB}, is somewhat unusual for this type of complex. That is, although the nuclear barrier for ET is enough high to trap the electronic states, the energy split due to resonance at the crossing point is also enough large to promote a relatively fast ET, as revealed by the magnitude of k_{ET}.

Comparison between $[(bpy)_2ClRu(bta)RuCl(bpy)_2]^{2+}$ and $[(edta)Ru(bta)Ru(edta)]^{4-}$ [30–32] reinforced that the degree of electronic coupling for the latter is rather larger than the predicted and suggests that the system might be delocalized or near the delocalized-regime limit.

The difference in properties between bpy- and edta-containing dimers is striking. As emphasized before [59] and here observed, the activation barriers to make the donor (Ru^{II}) and acceptor (Ru^{III}) sites equivalent in $[(bpy)_2ClRu(L)RuCl(bpy)_2]^{n+}$ are relatively low: ~ 5.5 kcal mol^{-1} for L = pz [53] and ~ 3.2 kcal mol^{-1} for L = bta, both determined by measurements of IVCT bands in acetonitrile at room temperature. Because of the discrete values, the transition from slight to large or even full delocalization is small energetically and can be promoted by enhancing orbital overlap at expense of subtle chemical modifications, as in the case of the replacement of the ancillary ligands bpy with edta.

The fact that $[(bpy)_2ClRu(bta)RuCl(bpy)_2]^{2+}$ is thermodynamically favored with respect to $[(edta)Ru(bta)Ru(edta)]^{4-}$ (on the basis of K_c [30]) has to be interpreted with care and, herein, can be explained in terms of the directional, synergistic interactions of the type $Ru^{II} \rightarrow L_b$ MLCT and $L_b \rightarrow Ru^{III}$ LMCT, which appear to be more effective in the former case. Hence, one may conclude that the comproportionation energy (from $\Delta E_{1/2}$) itself is not very expressive upon comparing intermetallic electronic couplings for different systems, since ΔG_c is composed of, at least, four terms [16,49]. In the cases with weak coupling, the delocalization term, ΔG_d, is practically negligible if compared to the synergistic term, ΔG_s (which comprises the cooperative charge-transfer and backbonding interactions, and the π-acid/base effects). In the delocalized cases, on the other hand, ΔG_d predominates due to the absence of vectorial (dipole-oriented) interactions.

Besides electronic interactions, the specific example of $[(edta)Ru(bta)Ru(edta)]^{4-}$ involves a dynamic, structural factor (fluxionality) which also makes the metal–metal distance shorter and enhances the orbital overlap between the redox sites by mixing with ligand orbitals of the appropriate symmetry, as discussed elsewhere [31,32]. There is still concerns about whether this system is partially localized or fully delocalized. Insight into this issue can be gained by the comparisons provided above, where regardless of belonging to a class III or an intermediate class II/III regime, clearly its mixed-valence properties cannot be predicted by Hush's theory for weakly or moderately interacting systems.

The twofold comparisons made herein between the mixed-valence features of (i) $[(bpy)_2ClRu(bta)RuCl(bpy)_2]^{2+}$ and $[(bpy)_2ClRu(pz)RuCl(bpy)_2]^{3+}$, or (ii) $[(bpy)_2ClRu(bta)RuCl(bpy)_2]^{2+}$ and $[(edta)Ru(bta)Ru(edta)]^{4-}$, also reinforce the idea that the extent of metal–metal and electronic/charge-transfer interactions between ligand-bridged donor–acceptor complexes can be varied (or modulated) by a series of replacements or relatively simple chemical modifications either (i) on the intervening bridging ligand or (ii) on the non-bridging (ancillary) ligands surrounding the metal ions.

Lastly, it is worth noting that pyridine, pyrazine, and pyrimidine derivatives [17,70] are usually electron-poor type ligands and mediate metal–metal interactions through low-lying π* orbitals (LUMOs) by invoking electron-transfer mechanisms [56]. By contrast, electron-rich anionic bridging ligands, such as imidazolate and triazolate derivatives[13] intercede intermetallic interactions via hole-transfer mechanisms, taking advantage of relatively high-lying filled molecular orbitals (HOMOs) [56]. Dinuclear mixed-valent complexes of the latter sort of ionizable ligands as bridges are of interest because their proton-coupled ET [75] properties can be subjected to fine-tuning by control of pH [14]. Indeed, we have recently reported an interesting case of proton-induced electron-coupling switching and related phenomena based on a benzotriazolate-bridged system [30].

Acknowledgements

The support from the Brazilian agencies CNPq and FAPESP is gratefully acknowledged.

[12] A more realistic k_{ET} value for such systems could in principle be assessed by means of IR spectroscopy, on the basis of the coalescence of the vibrational bands [68,69]. However, unlike systems involving ligands with typical, well-defined vibrational markers (e.g. CO [69]), in this particular case it has not been possible to discuss the degree of delocalization based on the IR bands of bta, since the bands associated to the acetate (edta) modes obscure the weaker bands of the bridging ligand.

[13] To cite only a few literature references, see recent works by Haga [71], Nag [72], Pickup [73], Vos [74], and co-workers).

References

[1] R.C. Rocha, H.E. Toma, Quim. Nova 25 (2002) 624 (references cited therein).
[2] K. Prassides (Ed.), Mixed Valency Systems: Applications in Chemistry, Physics and Biology, NATO ASI Series (C-343), Kluwer, Dordrecht, 1991.
[3] D.B. Brown (Ed.), Mixed-Valence Compounds: Theory and Applications in Chemistry, Physics, Geology, and Biology, Proceedings of the NATO Advanced Study Institute, Reidel, Dordrecht, 1980.
[4] G.C. Allen, N.S. Hush, Prog. Inorg. Chem. 8 (1967) 357.
[5] N.S. Hush, Electrochim. Acta 13 (1968) 1005.
[6] N.S. Hush, Prog. Inorg. Chem. 8 (1967) 391.
[7] R.S. Mulliken, W.B. Person, Molecular Complexes, Wiley, New York, 1969.
[8] R.S. Mulliken, J. Am. Chem. Soc. 74 (1952) 811.
[9] M.B. Robin, P. Day, Adv. Inorg. Chem. Radiochem. 10 (1967) 247.
[10] D.O. Cowan, C. Levanda, J. Park, F. Kaufman, Accounts Chem. Res. 6 (1973) 1.
[11] D.O. Cowan, F. Kaufman, J. Am. Chem. Soc. 92 (1970) 219.
[12] C. Creutz, H. Taube, J. Am. Chem. Soc. 95 (1973) 1086.
[13] C. Creutz, H. Taube, J. Am. Chem. Soc. 91 (1969) 3988.
[14] M.D. Ward, Chem. Soc. Rev. 24 (1995) 121.
[15] R.J. Crutchley, Adv. Inorg. Chem. Rad. 41 (1994) 273.
[16] C. Creutz, Prog. Inorg. Chem. 30 (1983) 1.
[17] V. Balzani, A. Juris, M. Venturi, S. Campagna, S. Serroni, Chem. Rev. 96 (1996) 759.
[18] L. De Cola, P. Belser, Coord. Chem. Rev. 177 (1998) 301.
[19] H.E. Toma, An. Acad. Bras. Cienc. 72 (2000) 5.
[20] C. Joachim, J.K. Gimzewski, A. Aviram, Nature 408 (2000) 541.
[21] M.A. Fox, Accounts Chem. Res. 32 (1999) 201.
[22] P. Belser, S. Bernhard, C. Blum, A. Beyeler, L. De Cola, V. Balzani, Coord. Chem. Rev. 192 (1999) 155.
[23] A. Harriman, R. Ziessel, Coord. Chem. Rev. 171 (1998) 331.
[24] D. Astruc, Accounts Chem. Res. 30 (1997) 383.
[25] J. Jortner, M. Ratner (Eds.), Molecular Electronics, Blackwell Science, Malden, 1997.
[26] J.-M. Lehn, Supramolecular Chemistry: Concepts and Perspectives, VCH, Weinheim, 1995.
[27] A.J. Bard, Integrated Chemical Systems: A Chemical Approach to Nanotechnology, Wiley, New York, 1994.
[28] J.-M. Lehn, Angew. Chem., Int. Ed. Engl. 27 (1988) 89.
[29] F.L. Carter (Ed.), Molecular Electronics, Marcel Dekker, New York, 1987.
[30] R.C. Rocha, H.E. Toma, Inorg. Chem. Commun. 4 (2001) 230.
[31] R.C. Rocha, H.E. Toma, Inorg. Chim. Acta 310 (2000) 65.
[32] R.C. Rocha, K. Araki, H.E. Toma, Inorg. Chim. Acta 285 (1999) 197.
[33] R.C. Rocha, Ph.D. Thesis, Universidade de São Paulo, São Paulo, 2000.
[34] R.C. Rocha, H.E. Toma, Transition Met. Chem. 28 (2003) 43.
[35] H.E. Toma, R.C. Rocha, Croat. Chem. Acta 74 (2001) 499.
[36] R.C. Rocha, K. Araki, H.E. Toma, Transition Met. Chem. 23 (1998) 13.
[37] H.E. Toma, E. Giesbrecht, R.L.E. Rojas, J. Chem. Soc., Dalton Trans. (1985) 2469.
[38] H.E. Toma, E. Giesbrecht, R.L.E. Rojas, Can. J. Chem. 61 (1983) 2520.
[39] R.C. Rocha, H.E. Toma, Can. J. Chem. 79 (2001) 145.
[40] B.P. Sullivan, D.J. Salmon, T.J. Meyer, Inorg. Chem. 17 (1978) 3334.
[41] D.T. Sawyer, J.L. Roberts, Jr., Experimental Electrochemistry for Chemists, Wiley, New York, 1974, p. 212.
[42] A.L. Bard, L.R. Faulkner, Electrochemical Methods: Fundamentals and Applications, 2nd ed., Wiley, New York, 2000.
[43] D.J.G. Ives, G.J. Janz, Reference Electrodes: Theory and Practice, Academic Press, New York, 1961.
[44] F.N. Rein, R.C. Rocha, H.E. Toma, J. Coord. Chem. 53 (2001) 99.
[45] H.E. Toma, R.M. Serrasqueiro, R.C. Rocha, G.J.F. Demets, H. Winnischofer, K. Araki, P.E.A. Ribeiro, C.L. Donnici, J. Photochem. Photobiol. A 135 (2000) 185.
[46] M. Franco, K. Araki, R.C. Rocha, H.E. Toma, J. Solution Chem. 29 (2000) 667.
[47] M.J. Powers, T.J. Meyer, Inorg. Chem. 17 (1978) 2955.
[48] B.P. Sullivan, D. Conrad, T.J. Meyer, Inorg. Chem. 24 (1985) 3640.
[49] D.E. Richardson, H. Taube, Coord. Chem. Rev. 60 (1984) 107.
[50] J.E. Sutton, H. Taube, Inorg. Chem. 20 (1981) 3125.
[51] J.E. Sutton, P.M. Sutton, H. Taube, Inorg. Chem. 18 (1979) 1017.
[52] J.N. Braddock, T.J. Meyer, Inorg. Chem. 12 (1973) 723.
[53] R.W. Callahan, F.R. Keene, T.J. Meyer, D.J. Salmon, J. Am. Chem. Soc. 99 (1977) 1064.
[54] R.W. Callahan, T.J. Meyer, Chem. Phys. Lett. 39 (1976) 82.
[55] R.C. Rocha, H.E. Toma, Polyhedron 21 (2002) 2089.
[56] G. Giuffrida, S. Campagna, Coord. Chem. Rev. 135 (1994) 517.
[57] M.D. Newton, Chem. Rev. 91 (1991) 767.
[58] C. Creutz, P. Kroger, T. Matsubara, T.L. Netzel, N. Sutin, J. Am. Chem. Soc. 101 (1979) 5442.
[59] T.J. Meyer, Accounts Chem. Res. 11 (1978) 94.
[60] N.S. Hush, J. Electroanal. Chem. 470 (1999) 170.
[61] R.A. Marcus, Angew. Chem., Int. Ed. Engl. 32 (1993) 1111.
[62] R.A. Marcus, Rev. Mod. Phys. 65 (1993) 599.
[63] R.A. Marcus, N. Sutin, Biochim. Biophys. Acta 811 (1985) 265.
[64] R.A. Marcus, Electrochim. Acta 13 (1968) 995.
[65] R.A. Marcus, Annu. Rev. Phys. Chem. 15 (1964) 155.
[66] R.A. Marcus, Discuss. Faraday Soc. 29 (1960) 21.
[67] N. Sutin, Prog. Inorg. Chem. 30 (1983) 441.
[68] K.D. Demadis, C.M. Hartshorn, T.J. Meyer, Chem. Rev. 101 (2001) 2655.
[69] T. Ito, T. Hamaguchi, H. Nagino, T. Yamaguchi, J. Washington, C.P. Kubiak, Science 277 (1997) 660.
[70] A. Juris, V. Balzani, F. Barigelletti, P. Belser, A. von Zelewsky, Coord. Chem. Rev. 84 (1988) 85.
[71] M. Haga, T. Ano, K. Kano, S. Yamabe, Inorg. Chem. 30 (1991) 3843.
[72] S. Baitalik, U. Florke, K. Nag, Inorg. Chem. 38 (1999) 3296.
[73] C.G. Cameron, P.G. Pickup, J. Am. Chem. Soc. 121 (1999) 11773.
[74] R. Hage, J.G. Haasnoot, J. Reedijk, R.Y. Wang, J.G. Vos, Inorg. Chem. 30 (1991) 3263.
[75] S.J. Spencer, J.K. Blaho, J. Lehnes, K.A. Goldsby, Coord. Chem. Rev. 174 (1998) 391.